Functionalization Effects of Single-Walled Carbon Nanotubes as Templates for the Synthesis of Silica Nanorods and Study of Growing Mechanism of Silica

Kyoung G. Lee,[†] Rinbok Wi,[†] Muhammad Imran,[†] Tae Jung Park,[‡,*] Jaebeom Lee,[§] Sang Yup Lee,[†,‡] and Do Hyun Kim[†,*]

[†]Department of Chemical & Biomolecular Engineering (BK21 program), and Center for Ultramicrochemical Process Systems, KAIST, 335 Gwahangno, Yuseong-gu, Daejeon 305-701, Republic of Korea, [‡]Bioprocess Engineering Research Center, Center for Systems & Synthetic Biotechnology, and Institute for the BioCentury, KAIST, 335 Gwahangno, Yuseong-gu, Daejeon 305-701, Republic of Korea, and [§]Department of Nanomedical Engineering, Pusan National University, 50 Cheonghak-ri, Samrangjin-eup, Miryang-si 627-706, Republic of Korea

ABSTRACT Silica nanorods were successfully prepared through a sol−gel process in the presence of carboxylic-functionalized single-walled carbon nanotubes (C-SWCNTs). The effect of chemical functionalization of single-walled carbon nanotubes (SWCNTs) on the growth of the silica layer was investigated using pristine SWCNTs (P-SWCNTs) and C-SWCNTS. The C-SWCNTs served as a unique template to fabricate silica hybrid composite materials. The crystalline formation and growing mechanism of the silica layer on C-SWCNTs were explained by the hydrolysis and chemical bonding between silica precursors and carboxylated SWCNTs. The C-SWCNTs, as templates, were successfully encapsulated using silica, and used templates were removed by oxidation at high temperature. Finally, silica nanorods/nanowires were synthesized in forms of mold, and this silica fabrication mechanism could be applied for large-scale production of silica nanomaterials and highly flexible nanocomposites. The sequence of a silica encapsulation process of C-SWCNTs and removed C-SWCNTs was characterized using SEM, TEM, EDX, FT-IR and Raman spectroscopy, XRD, and electrical analysis.

KEYWORDS: silica nanorod · single-walled carbon nanotube · sol−gel

One-dimensional (1D) nanomaterials including nanotubes, nanorods, and nanowires have brought great interests over the past decades due to their unique mechanical, electrical, and optical properties.[1,2] These particular dimensional advantages of 1D nanomaterials allow for a variety of nanostructure applications, including high-strength nanocomposites, field-emitting surfaces, sensors, nanotransistors, biomaterial delivery tools, sensors, optic devices, electrode materials, energy storage devices, and catalysis materials.[3−12] Many 1D nanomaterials such as cerium oxide nanotube, zinc oxide nanotubes, gold nanorods, carbon nanotubes (CNT), and silicon nanowires have been fabricated and reported recently.[13−17] Among these different types of 1D nanomaterials, the silica nanorod has gained interest due to its distinct optical, electrical, and mechanical properties.[18] Additionally, silica nanorods possess a large surface area, are easily incorporated with other nanomaterials, and possess high biocompatibility, which provide unique properties suitable for catalysis, nanosensors, drug and gene delivery applications.[19]

Recently, numerous methods such as vapor phase deposition, surfactant stabilization, and anodized aluminum oxide (AAO) have been developed to fabricate silica nanorods. Adachi and co-workers proposed a surfactant-mediated technique for preparing silica nanotubes.[20] This proposed method selected the laurylamine hydrochloride (LAHC, surfactant)/tetraethyl orthosilicate (TEOS) system, which controls the molar ratio of LAHC and TEOS to manipulate the diameter and length of silica nanotubes. Whitsitt and Barron also fabricated silica and CNT nanocomposite materials by adopting fluorosilicic acid and surfactant, sodium dodecyl sulfate (SDS) or dodecyl trimethylammonium bromide (DTAB), to coat the surface of the CNT.[21] However, these methods require an optimized surfactant to TEOS ratio, which is difficult to find, and require extra washing steps to remove the surfactant due to the toxicity for further applications. The AAO method utilizes an AAO membrane, which has a uniform diameter, as a template for preparation of a silica nanotube.[22] However, it is difficult to control the diameter and length of the silica nanorods using the AAO method. Silica nanotubes were also synthesized using

*Address correspondence to tjpark@kaist.ac.kr, dohyun.kim@kaist.ac.kr.

Received for review April 18, 2010 and accepted June 07, 2010.

Published online June 10, 2010. 10.1021/nn100807r

various metal powders as initiating materials under high temperature and pressure to grow as 1D nanostructure materials.[23−26] These methods also have technical challenges in controlling the diameter of silica nanorods and require high temperature, high pressure, and expensive equipment for a large-scale production.

For these reasons, the template-assisted method has been an attractive and popular choice as an alternative method to overcome these problems. Several inorganic 1D nanomaterials including Ag nanowires, Au nanorods, and $V_3O_7 \cdot H_2O$ nanowires have been employed as templates to synthesize silica nanotubes due to their easy removal of the templates under alkaline or acidic conditions.[27−29] These introduced templates provide binding sites for the silica formation, and the diameter of the silica can be controlled by the reaction time, temperature, or the molar ratio of the TEOS. However, this still does not address the major challenges of using these 1D nanomaterials as templates, which are the handling of toxic organic chemicals or surfactants and the difficulties of controlling their shape and size. Due to these reasons, CNTs have been the focus as candidate materials for the template. CNTs are also considered as the most significant platforms for the fabrication of 1D nanomaterials due to the uniform size and shape with great mechanical and chemical stabilities. Recently, a silica−CNT nanocomposite has attracted great attention due to the synergetic effect of both CNTs and silica, which provides an excellent platform in biological, electrical, optical, and catalysis applications.[30] Despite large surface area and great electrical and mechanical properties, CNTs have numerous issues in biological applications, such as poor dispersion, toxicity, and difficulties in functionalization. Silica is a well-known inert support material for adopting other nanoparticles in catalysis application. However, it is difficult to fabricate one-dimensional structures using silica, such as nanorods and nanowires. The combination of CNT and silica would produce unique hybrid silica−CNT nanorods that solve the issues of using CNTs alone in various applications. Several methods have been reported to fabricate the silica-coated CNT nanocomposite using noncovalently or covalently functionalized CNTs and direct coupling of silica nanoparticles with CNTs.[31,32] However, in most cases, it is difficult to obtain a uniform silica coating over CNTs due to the lack of chemical affinities between silica and the CNT.

The functionalization of CNTs has been conventionally employed using strong acid, such as a mixture of sulfuric acid (H_2SO_4) and nitric acid (HNO_3).[32] It has been known that this modification assists in the adsorption of silica nanoparticles on CNTs. In this study, we demonstrate the synthesis of silica nanorods through the modified Stöber sol−gel process using functionalized single-walled carbon nanotubes (SWCNTs) as a template. SWCNTs are great templates because of a large surface area, high aspect ratio, and great chemical and mechanical stabilities. Due to the different interaction between pristine SWCNTs (P-SWCNTs) or functionalized SWCNTs with TEOS, the morphology of the resulting material was also different. Growth and formation mechanism of the silica network and effects of the surface modification of the SWCNTs on the fabrication of silica nanorods were mainly discussed. Furthermore, the formation of the typical silicon oxide (SiO_2) structures during the silica growing over SWCNTs *via* the sol−gel method is observed and reported for the first time.

RESULTS AND DISCUSSION

Effects of Chemical Functionalization of SWCNTs on the Synthesis of Silica Nanorods. The diameter of individual P-SWCNT is in the range of 0.9−1.2 nm, but it exists as bundles due to the strong agglomeration between P-SWCNTs (see Figure S1 in Supporting Information).[34] To the best of our knowledge, there has been no report about the effects of chemical functionalization of SWCNTs for the formation of a silica layer and its growing mechanisms on the surface of a carbon nanotube. The understanding of the effects of chemical functionalization of SWCNTs and the mechanism of silica growth on SWCNTs is important to control the morphology and properties of silica−SWCNT nanocomposite materials.

The effects of silica formation on both P-SWCNTs and carboxyl-functionalized SWCNTs (C-SWCNTs) are investigated using the sol−gel method. It has been known that P-SWCNTs are difficult for modifying or fabricating various types of nanocomposite materials because of the low affinity of P-SWCNTs with other nanoparticles.[34,35] However, chemically functionalized SWCNTs can be more easily modified with other organic or inorganic nanomaterials to achieve high affinity with nanoparticles.[33] In order to investigate chemical functionalization effects of CNTs on the growth of silica, both P-SWCNTs and C-SWCNTs are treated as templates under same conditions. The morphology changes of silica growth and coating over P-SWCNTs and C-SWCNTs were investigated using scanning electron microscopy (SEM). The overall silica formation process of C-SWCNTs is proposed in Scheme 1. The confirmation of carboxyl group formation on SWCNTs is discussed further in the next section.

After 1 h of chemical reactions, silica nanoparticles and P-SWCNTs existed separately and the P-SWCNTs appeared as bundles, as shown in Figure 1a. Most P-SWCNTs remained as forms of bundles, and separate aggregates of silica nanoparticles were synthesized even after further reactions, as shown in Figure 1b. After 24 h of chemical reaction, P-SWCNTs were still observed as bundles and the silica nanoparticles were aggregated around the surface of P-SWCNTs (Figure 1c, and see Figure S2 in Supporting Information). On the other hand, synthesized silica nanoparticles were de-

posited over C-SWCNTs and uniformly coated to produce 1D nanostructure materials (Figure 1d). With additional reaction time, the diameter of silica nanorods@C-SWCNTs increased and the final C-SWCNTs were uniformly coated with silica that leads to the formation of a 1D silica@C-SWCNT nanocomposite (Figure 1e,f).

These results proved that the chemically modified C-SWCNTs provide a bonding site for the adsorption of silica precursors and created silica layers over the surface of C-SWCNTs. However, the P-SWCNT has an inefficient chemical binding affinity between silica precursors and CNTs that prevents the growth of silica layers on the surface of P-SWCNTs.[36] For these reasons, it is important to control the morphology and characteristics of silica hybrid nanomaterials for the surface modification of SWCNTs as templates.

Growing Mechanism of Silica Nanorods. The P-SWCNTs were chemically modified using the acid mixture to obtain C-SWCNTs (see Figure S3 in Supporting Information). As discussed before, the modified surface can provide a binding site between silica precursors and C-SWCNTs. Once the silica precursors attached on the surface of C-SWCNTs, additional silica precursors are adsorbed next to the previously grown silica layers and are involved in further silica growth reactions. After silica@C-SWCNTs were obtained, the C-SWCNT templates can be removed by oxidation of carbon with air at high temperature to generate carbon dioxide gas (CO_2), leaving a hollow structure inside the silica nanorods.

From the obtained silica@C-SWCNT 1D nanomaterials, six types of possible mechanisms could be observed and proposed as follows: (1) partial silica coating over C-SWCNT, (2) partial silica coating over two C-SWCNTs, (3) partial silica coating over the C-SWCNT bundle, (4) silica encapsulation of C-SWCNT, (5) silica encapsulation of two-stranded C-SWCNTs, and (6) silica encapsulation of the C-SWCNT bundle. These proposed six silica growth models are well-illustrated in Scheme 1 and are possibly observed in the microscope images of the silica@C-SWCNT product, as shown in Figure 2a−f. These proposed mechanisms might be explained from the chemical functionalization and unique characteristics of SWCNTs. In case of P-SWCNT, it shows a high tendency to exist as bundles due to the strong attraction between SWCNTs. In this experiment, P-SWCNTs were chemically modified using an acid mixture, and carboxylic groups were produced on the surface of P-SWCNTs. The fabricated C-SWCNTs were dispersed using ultrasound in the mixture of ethanol and water to prevent agglomeration between SWCNTs. However, partial amounts of C-SWCNTs were well-dispersed in the solution, and most of C-SWCNTs still existed as double strands or bundles. In this case, the properly dispersed single strand of the C-SWCNT was separately encapsulated by silica but poorly dispersed C-SWCNTs resulted in silica containing double strands or bundles of

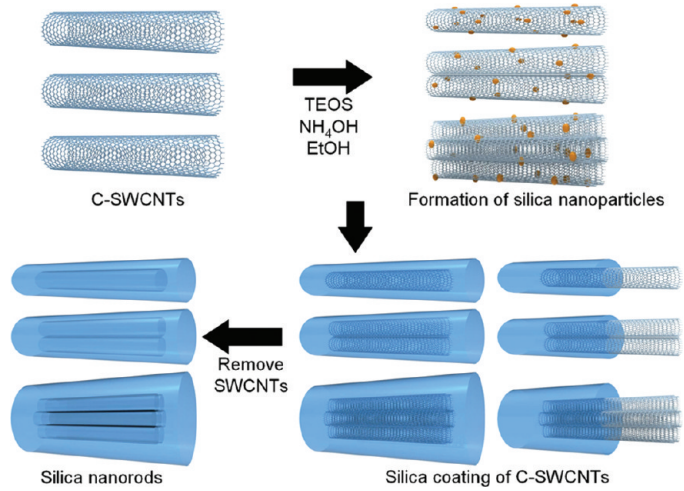

Scheme 1. Schematic illustration of the formation process of silica nanorods from C-SWCNTs.

C-SWCNTs during the reaction (Figure 2b,c,e,f). In addition, partial silica encapsulation and perfect silica encapsulation of C-SWCNTs are also observed, as shown in Figure 2a−f. These results might be explained from the functionalization of SWCNTs. From the previous results about the effect of chemical modification of SWCNTs to the silica growing, almost no P-SWCNTs were encapsulated by silica due to the low silanization effects between P-SWCNTs and silica precursors. On the contrary, it is clearly shown that carboxyl formation of the surface of SWCNTs could increase the silanization rate with TEOS, as indicated by the silica growing over the surface of C-SWCNTs. Therefore, it is highly believed that the carboxyl functional groups might not be formed on the end of P-SWCNTs. A small number of carboxyl functional groups on the end of C-SWCNTs might provide fewer chemical binding sites for employing silica layers and results in partial silica coating over C-SWCNTs. In order to understand the silica growing mechanism, the morphology changes of silica@C-SWCNTs were examined in 15 min intervals. After 15 min of chemical reaction, double strands or bundles of C-SWCNTs with an individual diameter about 1.2 nm were observed, as shown in Figure 2g (see Figure S4 in Supporting Information). There are small roughness changes on the surface of C-SWCNTs, but it is hard to distinguish between C-SWCNTs and silica precursors. After 30 min of reaction, silica grew and encapsulated the C-SWCNT, as shown in Figure 2h. The inner diameter was 1.2 nm, which is in the diameter range of employed C-SWCNTs, and thin silica layers grew on the surface of the C-SWCNT with 0.28 nm thickness of individual silica layer-by-layer in a short period (Figure 2h). However, in most of the cases, these thin silica subnanolayers appeared limitedly and partially during the silica growing process, which exhibited well-defined typical SiO_2 structures with the interplanar lattice distance of 3.864 ± 0.171 Å and showed {111} orthorhombic structure (Figure 2g,h, and see Figure S5 in Support-

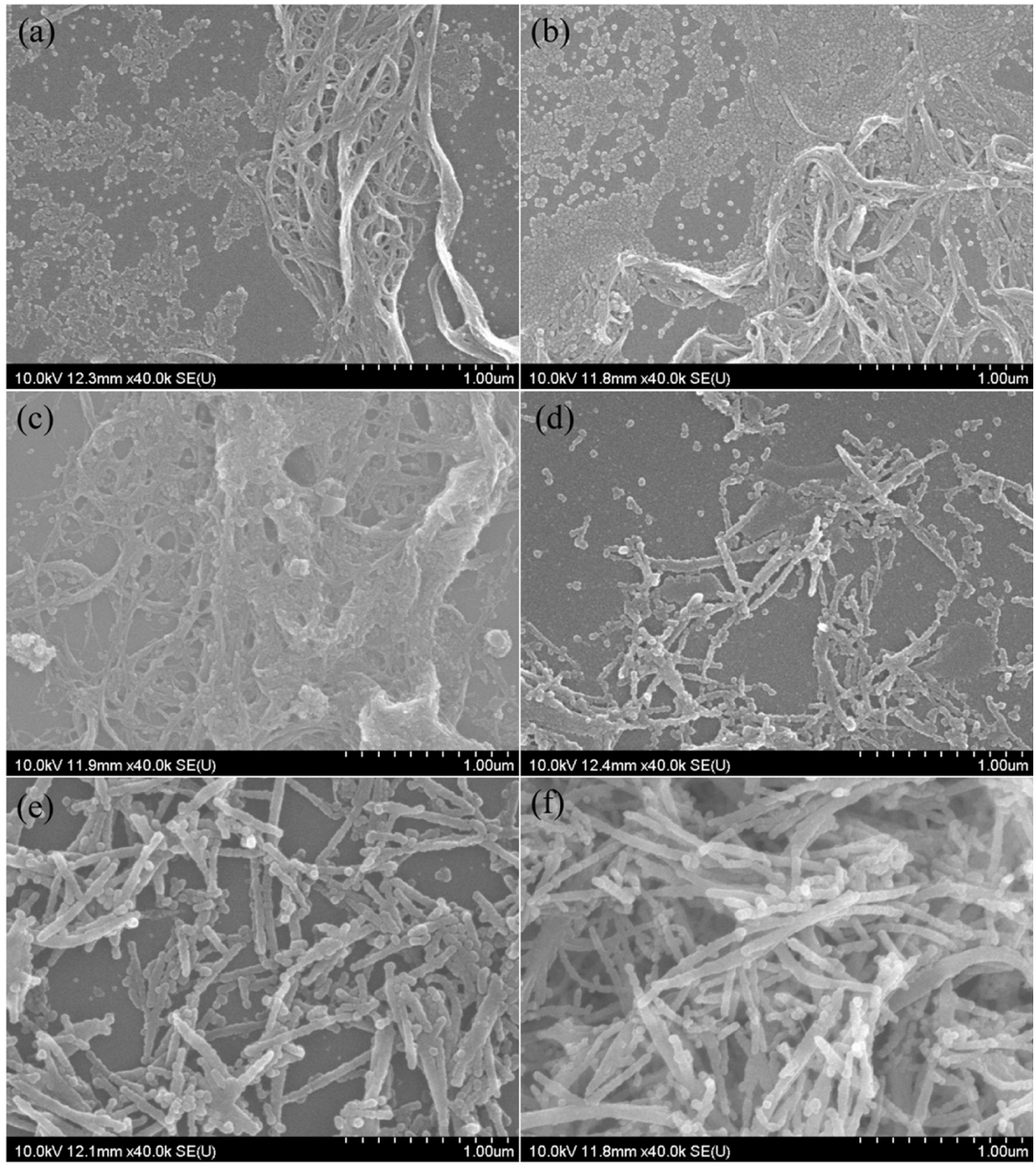

Figure 1. Typical SEM images of silica growing on the P-SWCNTs at different reaction times of (a) 1 h, (b) 2 h, and (c) 24 h. Typical SEM images of same reaction conditions as P-SWCNTs except using C-SWCNTs at different reaction times of (d) 1 h, (e) 2 h, and (f) 24 h.

ing Information).[37] These observed data show a unique behavior of the silica growing process. In most of the cases, it is known that silica is fabricated as an amorphous material due to the random growing of silica precursors. It is believed that silica precursors are deposited on the surface of C-SWCNTs and grow in an axial direction for certain thickness, and it would disappear because of the random growing direction of the silica precursors and different silica hydrolysis and deposition rate. After 45 min of reaction, most of C-SWCNTs are covered by a layer of silica, and the coated silica shows amorphous structures (Figure 2i, and see Figure S6 in Supporting Information).

The C-SWCNTs act as a frame material for deposition of silica precursors to fabricate silica nanorods. The hydrolysis of TEOS continuously occurs and produces silica precursors to be intact with the outermost surface of C-SWCNTs. As silica nanoparticles were growing, most portions of the C-SWCNTs were covered with silica (see Figure S7 in Supporting Information). During this process, both individual and bundled C-SWCNTs were covered with silica to make a 1D particle. After the reaction was over, the residual template C-SWCNT was removed by oxidation under high temperature in the presence of air for several hours. The diameter of the fabricated silica@C-SWCNTs is 62.8 $\pm$ 10.9 nm, which

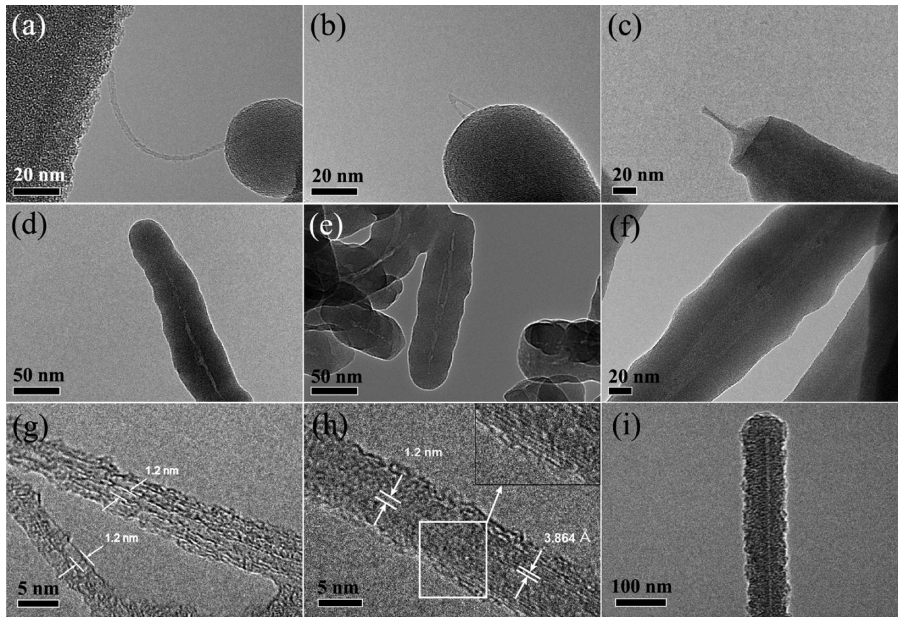

Figure 2. Typical partial silica coating TEM images of (a) single C-SWCNT, (b) double strands of C-SWCNTs, and (c) bundle C-SWCNTs. Typical perfect silica coating TEM images of (d) single C-SWCNT, (e) double strands of C-SWCNTs, and (f) bundle C-SWCNTs. Silica growing process of (g) 15 min of reaction, (h) 30 min of reaction, and (i) 45 min of reaction.

was observed with more than 100 counts from transmission electron microscopy (TEM) images. The typical hollow structure of silica nanorods is observed in TEM images, as shown in Figure 3b, with similar diameters of silica@C-SWCNTs. The inner surface of the silica nanorods is relatively smooth, and the inner diameter ranged from 2 to 30 nm. The inner diameter of the silica nanorods is dependent on the number of C-SWCNTs encapsulated by the silica shell.

The above results show that the inner diameter of silica nanorods can be controlled by adjusting the number of SWCNTs. The fabricated silica nanorods with uniform size and shape after removing C-SWCNTs are observed using SEM, as shown in Figure 3a,b. From the obtained TEM and SEM images, both ends of the silica nanorods are completely closed during the calcination process. Figure 3c shows the energy-dispersive X-ray spectrum (EDX) analysis of silica nanorods after removing C-SWCNTs. Three distinct peaks of oxygen, silicon, and aluminum from silica nanorods are observed from the EDX analysis, and the aluminum signal originates from the substrate. This result further confirmed that the carbon atoms of C-SWCNTs as templates were reacted with oxygen (O_2) in the presence of air and converted to carbon monoxide (CO) or carbon dioxide (CO_2) gas under the high temperature. As a result, the use of SWCNTs allows the growth of silica nanoparticles on the surface of nanotubes. The synthesized silica nanorods were fabricated without distortion or decomposition of their structures during the process, and nanorods have an amorphous structure.

Optical Analysis. The P-SWCNTs, C-SWCNTs, silica nanorods@SWCNTs, and silica nanorods were investigated using Raman spectroscopy, and the results are presented in Figure 4a. The Raman spectra show almost no peak shifts in the disorder-induced band (D-band) and the tangential band (G-band) before and after acid treatment of SWCNTs and silica coating. The Raman spectra of C-SWCNTs did show that the intensity of the radial breathing modes (RBMs) in the range of 250−400 cm^{-1} decreased after acid treatment of SWCNTs due to the structural changes and formation of the carboxyl group (COOH) on the surface.[33] The D-band provides an idea for understanding the disruptions in the hexagonal framework and the structure change of sp^2 carbon and sp^3 carbon of SWCNTs.[38,39] After the mixture acid treatment on SWCNTs, the intensity of the D-band relatively increased due to the change in carbon atoms from sp^2 to sp^3, which is evidence of carboxyl functionalization. This spectra change of RBMs, D-band, and G-band between C-SWCNTs and silica nanorods@C-SWCNTs was not observed. These Raman spectra show that the structural properties of C-SWCNTs are well-preserved even after silica layer formation over the surface of C-SWCNTs. After the C-SWCNTs are completely removed, the significant Raman spectra change was observed in RBMs, D-band, and G-band. The RBMs, D-band, and G-band spectra are important and a unique signature to prove the existence of SWCNTs using Raman spectra. All of the RBMs, D-band, and G-band completely disappeared after removal of SWCNTs, indicating that almost all of the SWCNTs were destroyed and removed from the inside of the silica shell through the high-temperature oxidation process. This implies that C-SWCNTs are excellent templates to fabricate silica nanorods and are easily removed using a high-temperature oxidation process.

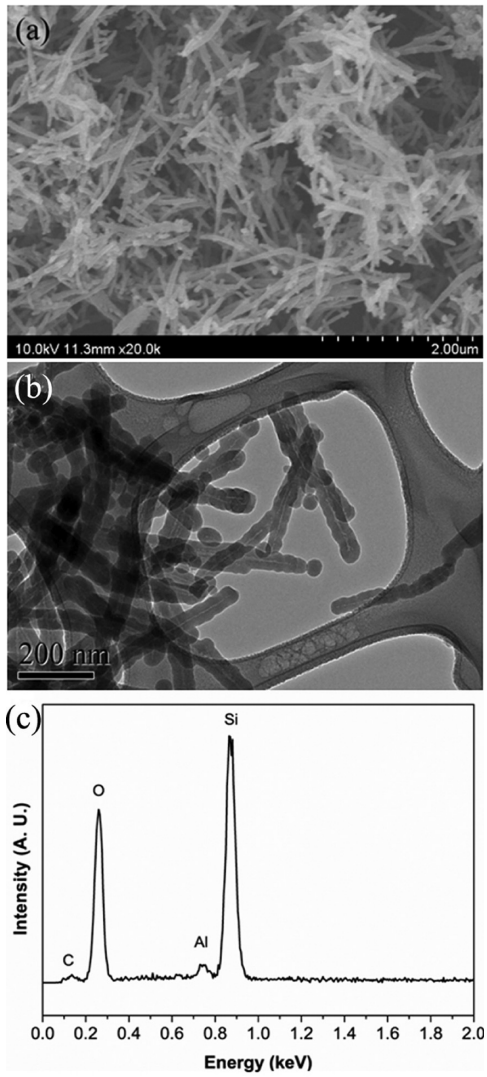

Figure 3. SEM (a) and TEM (b) images of silica nanorods. (c) EDX spectrum of silica nanorods on an aluminum substrate.

The P-SWCNTs, C-SWCNTs, silica@P-SWCNTs, silica@C-SWCNTs, and silica nanorods were investigated by Fourier transform infrared (FT-IR) spectroscopy (Figure 4b). The P-SWCNTs show no significant band observation, even after silica was employed, providing evidence that silica was not covered over the surface of P-SWCNTs. After the mixture acid treatment to P-SWCNTs, the carboxylic group in C-SWCNTs appeared at 1073 cm^{-1} (C−O−C and C−O vibrations), 1727 cm^{-1} (C═O stretching), and 2982 cm^{-1} (O−H) band to confirm the successful chemical functionalization.[40,41] After the successful silica coverage over C-SWCNTs, chemical structure (*i.e.*, carboxyl group) of C-SWCNTs would be changed, which can be observed through the FT-IR spectrum. After reaction of C-SWCNTs with TEOS, the two major bands at 1727 cm^{-1} (C═O) and 2982 cm^{-1} (O−H) disappeared. This evidence strongly supports that the carboxyl groups are converted into Si−O−C and silica layers are fabricated on the surface of C-SWCNTs (see Scheme S1 in Supporting Information). After calcination of silica@C-SWCNTs at a high temperature, the peaks for C═C vibration and C−O stretching disappeared and only Si−O−Si remained, indicating that C-SWCNTs are successfully removed and only the fabricated silica nanorods remain. X-ray diffraction patterns were also investigated to compare the structure of SWCNTs and silica nanorods in Figure 4c. In the experimental results, to prove the proper removal of SWCNTs inside the silica nanorods, both silica@P-SWCNTs and silica@C-SWCNTs show no significant peak changes compared with silica nanorods before and after silica coating of P-SWCNT and C-SWCNT due to the dominant XRD peaks from amorphous structures of silica. The peaks of P-SWCNTs are observed at the 2θ angle in the range of 10−30°. After removing SWCNTs, the peaks were slightly shifted and match the common amorphous silica structure.

Electrical Characterization. For the investigation of the elimination of SWCNTs from the silica nanorods, P-SWCNTs, C-SWCNTs, silica@P-SWCNTs, silica@C-SWCNTs, and silica nanorods were analyzed by electrical measurements on the gold-fabricated electrodes. Figure 4d shows the change in conductance of silica nanorods between the different nanostructures. C-SWCNTs show a lower conductivity compared to P-SWCNTs due to the defects of SWCNTs during acid treatment. SWCNTs and silica@SWCNTs have a similar conductivity, which means that the intact SWCNTs remain within silica nanorods. However, silica nanorods, after removing of SWCNTs, have no conductivity like intact silica materials do. This clearly demonstrated that SWCNTs were responsible for the change of electrical property in the silica@SWCNT nanocomposites, thereby allowing SWCNTs to be used as a conductive electron transfer material which is encapsulated by silica insulation. However, SWCNTs have obvious issues of toxicity and can only be applied in limited biological applications in small amounts. Because of this reason, the confirmation of complete removal of the SWCNTs after calcination due to the potential cytotoxicity issues is required and the electrical measurements can be used to investigate the complete elimination of SWCNTs inside the silica nanorods. The electrical measurements revealed that it completely removed the conductance after elimination of the encapsulated SWCNTs inside the silica nanorods. The SWCNTs and the silica materials can interact by chemical modification on the surface of SWCNTs as templates. Furthermore, the rapid growing mechanism of the silica was employed, and a simple heating process was also performed for the eliminating templates. Thus, this simple, rapid, and efficient formation of silica nanorods has achieved remarkable success in pure preparation of nanorods. Silica nanorod and its preparation method can be used as a powerful building block for potential varied applications.

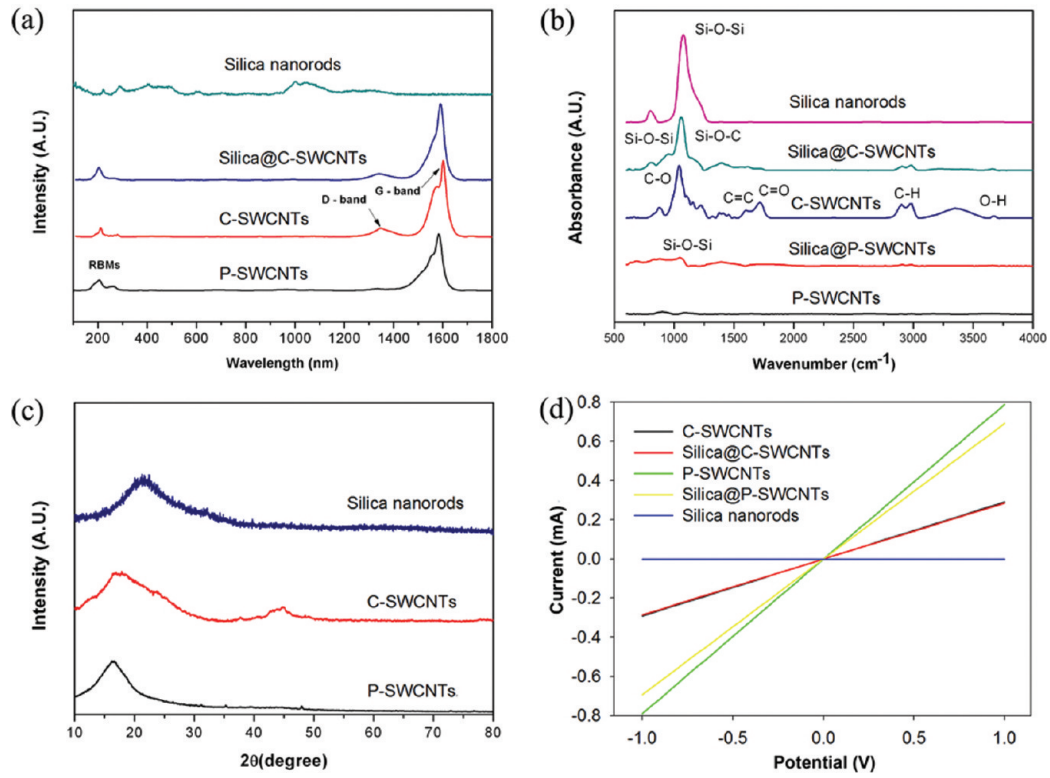

Figure 4. (a) Raman spectra of P-SWCNTs, C-SWCTNs, silica@C-SWCNTs, and silica nanorods. The intensities of P-SWCNTs, C-SWCNTs, and silica@C-SWCNTs were normalized on the G-band. (b) FT-IR spectra of P-SWCNTs, C-SWCNTs, silica@P-SWCNTs, silica@C-SWCNTs, and silica nanorods. (c) XRD patterns of P-SWCNTs, C-SWCNTs, and silica nanorods. (d) *I*—*V* curves using a probe station for the measurement of the electric current onto the gold electrodes at room temperature (black line, C-SWCNTs; red line, silica@SWCNTs; green line, P-SWCNTs; yellow line, silica@P-SWCNT; blue line, silica nanorods after removing SWCNTs).

Structure Influence of SWCNTs on the Silica Nanocomposite. Figure 5 shows the TEM images of a flexible silica@C-SWCNT nanocomposite. The fabricated silica@C-SWCNT was bent to make a U-shaped structure. The fabricated silica@C-SWCNT nanocomposite was not broken when it was bent. This indicated that the nanocomposite has excellent flexibility. In most of the cases, it is easy to modify the surface of silica but difficult to synthesize in its 1D shape. In contrast, SWCNTs have been known to be mechanically stable and highly flexible but difficult to modify the surface for further applications. This unique combining of properties demonstrates the advantages both silica and SWCNTs give to silica@C-SWCNT nanocomposites by providing highly stable and flexible nanocomposite materials, as observed in Figure 5a.

The tensile strength of silica-based nanorods can be predicted using strength measurement method, which is proposed by Meatthewson and his coworkers.[42] Due to the large amount of silica coated over C-SWCNTs, we only considered the Young's modulus (73.1 GPa) of silica and assumed that the Young's modulus of C-SWCNTs is negligible in calculating the theoretical tensile strength of silica@C-SWCNTs. Figure 5 shows the 40 nm diameter of the 1D silica@C-SWCNT that is flexibly bent to form a ribbon or alpha shape with a bending radius of 61 nm. Using the Young's modulus of silica, as shown in Figure 5b, our silica@C-SWCNTs would possess a theoretical tensile strength of at least 28 GPa, which is much better than the reported silica optical fibers.[43] This result also proves that the mechanical properties of both silica and C-SWNCTs are preserved and demonstrate high flexibility.

CONCLUSION

We have reported an effect of functionalization of SWCNTs during the synthesis of silica layers on the surface and coating of SWNTs. This proposed method is important to fundamentally understand how to fabricate silica nanorods by employing SWCNTs as templates. SWCNTs provide a high surface area and act as an excellent template for fabricating silica nanoparticles around C-SWCNTs to encapsulate them. The formation and fabrication mechanism of the silica shell over the SWCNT templates is proposed by the hydrolysis and chemical bonding between silica precursors and carboxylated SWCNTs. The SEM and TEM results showed that the affinity of silica nanoparticles depended on the chemical functionalization of SWCNTs. Unique structures and the high flexibility of silica nanorods were obtained when using SWCNTs as a template, displaying

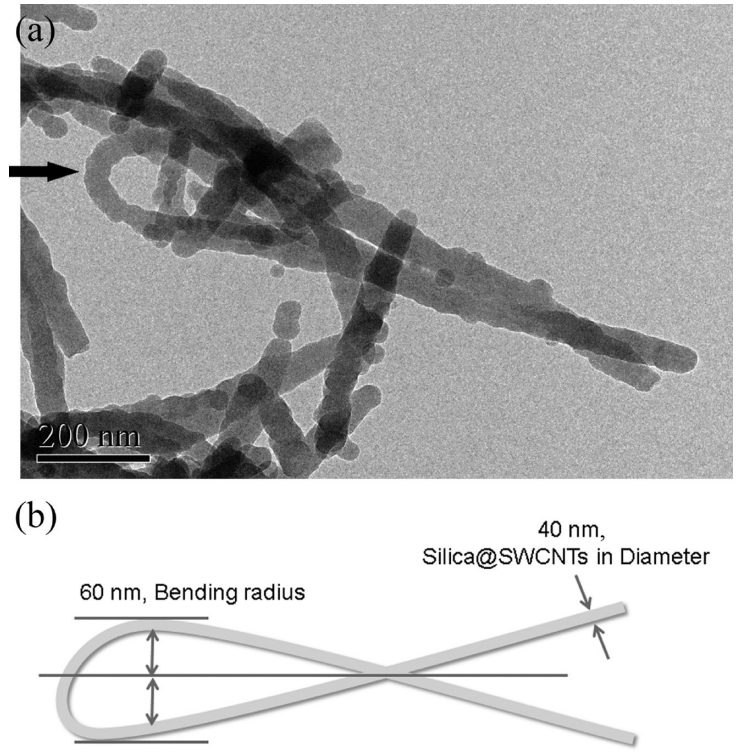

Figure 5. (a) TEM image of highly flexible silica@C-SWCNT nanocomposite. Black arrow represents the U-shaped structure of silica@C-SWCNT. (b) Geometry of the bent silica@C-SWCNT nanorod.

that the SWCNTs are good candidates for a stable template for fabricating one-dimensional structures. As a result, the proposed silica fabrication mechanism could be applied in a large-scale production of silica nanorods/nanowires and the synthesis of highly flexible nanocomposite materials.

EXPERIMENTAL SECTION

Materials. SWCNTs (Unidym) used here were synthesized by high-pressure carbon monoxide condensation. TEOS (98%), 3-aminopropyltriethoxysilane (APTS, 98%), ammonium hydroxide (28−30 wt %) were purchased from Sigma-Aldrich, and high-purity ethanol was obtained from Merck. All of the chemicals were used without further purification.

Synthesis of Silica Nanorods. P-SWCNTs were placed in hydrochloric acid and sonicated for 2 h to remove amorphous carbon and the metal catalyst. Purified SWCNTs were placed in a mixture of nitric acid and sulfuric acid (volume ratio of nitric acid and sulfuric acid = 2:9) under ultrasound treatment for 2 h and washed several times with deionized (DI) water. After acid treatment, the carboxyl groups were formed on the SWCNT surface. In order to compare the silica formation on P-SWCNTs and C-SWCNTs, 8 mg of P-SWCNTs or C-SWCNTs was dispersed in 40 mL of ethanol and 4 mL of DI water. After sonication of this mixture for 30 min, 0.32 g of TEOS and 0.5 mL of ammonium hydroxide were added and mixed for 24 h. The mixture was then centrifuged and washed several times with ethanol and DI water. Following the incubation of prepared silica@C-SWCNTs at 800 °C for 5 h, the SWCNTs were oxidized and removed during the heat treatment. The detailed process is demonstrated in Scheme 1.

Characterization of Silica Nanorods. The morphology of silica-coated SWCNTs was investigated using the field emission SEM (FE-SEM, Hitachi S4800) and the FE-TEM (JEOL JB-2100F). FT-IR spectroscopy was carried out IFS66 V/S & HYPERION 3000 (Bruker Optiks). The Raman spectra were obtained using a high-resolution dispersive Raman microscope (LabRAM HR UV/vis/NIR, Horiba Jobin Yvon).

Electrical Measurement. For the electrical measurement, a pulse ranging from −1.0 to 1.0 V was applied to the electrode using a manual probe station (SUMMIT 11862B), and current−voltage ($I-V$) was measured using a Keithley semiconductor characterization system (4200-SCS/F) on a manual probe station (Cascade) at room temperature. All SWCNTs, silica@SWCNTs, and silica nanorods with gold electrodes were prepared as follows. Prior to use, the Au electrodes were pretreated by first polishing with 0.05 μm alumina powder and then ultrasonically cleaned with DI water. All of the pretreated Au electrodes were dried at room temperature with nitrogen gas. SWCNTs, silica@SWCNTs, and silica nanorods were dispersed with DI water and prepared by filtering through an anodized membrane filter (47 mm in diameter, 0.2 μm pore size, Whatman). The resulting films were dried in the air and transferred on the Au electrode surface. Then, the filter membrane was melted by 3 M NaOH and washed out with DI water, subsequently. Following the drying under room temperature with vacuums, SWCNT/gold, silica@SWCNT/gold, and silica/gold electrodes were successfully fabricated for the electrical analysis.

Acknowledgment. This work was supported by the KOSEF through the Center for Ultramicrochemical Process Systems and WCU (World Class University) program through the National Research Foundation of Korea funded by the Ministry of Education, Science and Technology (R32-2008-000-10142-0). We would like to thank to the Korea Minting and Security Printing Corporation (KOMSCO).

Supporting Information Available: EDX mapping data of silica@C-SWCNTs and detailed TEM images of P-SWCNTs, C-SWCNTs, silica@P-SWCNTs, silica@C-SWCNTs are shown. Furthermore, acid treatment of P-SWCNTs and silanization of C-SWCNTs are illustrated. This material is available free of charge *via* the Internet at http://pubs.acs.org.

REFERENCES AND NOTES

1. Baughman, R. H.; Zakhidov, A. A.; de Heer, W. A. Carbon Nanotubes—The Route toward Applications. *Science* **2002**, *297*, 787–792.
2. Gupta, S.; Zhang, Q.; Emrick, T.; Russell, T. P. "Self-Corralling" Nanorods under an Applied Electric Field. *Nano Lett.* **2006**, *6*, 2066–2069.
3. Gue, S.; Li, J.; Renn, W.; Wen, D.; Dong, S.; Wang, E. Carbon Nanotube/Silica Coaxial Nanocable as a Three-Dimensional Support for Loading Diverse Ultra-High-Density Metal Nanostructures: Facile Preparation and Use as Enhanced Materials for Electrochemical Devices and SERS. *Chem. Mater.* **2009**, *21*, 2247–2257.
4. Ji, Q.; Iwaura, R.; Kogiso, M.; Jung, J. H.; Yoshida, K.; Shimizu, T. Direct Sol−Gel Replication without Catalyst in an Aqueous Gel System: From a Lipid Nanotube with a Single Bilayer Wall to a Uniform Silica Hollow Cylinder with an Ultrathin Wall. *Chem. Mater.* **2004**, *16*, 250–254.
5. Wei, B. Q.; Vajtai, R.; Jung, Y.; Ward, J.; Zhang, R.; Ramanath, G.; Ajayan, P. M. Assembly of Highly Organized Carbon Nanotube Architectures by Chemical Vapor Deposition. *Chem. Mater.* **2003**, *15*, 1598–1606.
6. Satishkumar, B. C.; Doorn, S. K.; Baker, G. A.; Dattelbaum, A. M. Fluorescent Single Walled Carbon Nanotube/Silica Composite Materials. *ACS Nano* **2008**, *2*, 2283–2290.
7. Norman, R. S.; Stone, J. W.; Gole, A.; Murphy, C. J.; Sabo-Attwood, T. L. Targeted Photothermal Lysis of the Pathogenic Bacteria, *Pseudomonas aeruginosa*, with Gold Nanorods. *Nano. Lett.* **2008**, *8*, 302–306.
8. Sun, B.; Sirringhaus, H. Surface Tension and Fluid Flow Driven Self-Assembly of Ordered ZnO Nanorod Films for High-Performance Field Effect Transistors. *J. Am. Chem. Soc.* **2006**, *128*, 16231–16237.
9. Kim, S.; Kim, S. K.; Park, S. Bimetallic Gold−Silver Nanorods Produce Multiple Surface Plasmon Bands. *J. Am. Chem. Soc.* **2009**, *131*, 8380–8381.
10. Fuhrer, M. S.; Kim, B. M.; Dürkop, T.; Brintlinger, T. High-Mobility Nanotube Transistor Memory. *Nano Lett.* **2002**, *2*, 755–759.
11. Zuttel, A.; Sudan, P.; Mauron, P.; Kiyobayashi, T.; Emmenegger, C.; Schlapbach, L. Hydrogen Storage in Carbon Nanostructures. *Int. J. Hydrogen Energy* **2002**, *27*, 203–212.
12. Huang, P. X.; Wu, F.; Zhu, B. L.; Gao, X. P.; Zhu, H. Y.; Yan, T. Y.; Huang, W. P.; Wu, S. H.; Song, D. Y. CeO_2 Nanorods and Gold Nanocrystals Supported on CeO_2 Nanorods as Catalyst. *J. Phys. Chem. B* **2005**, *109*, 19169–19174.
13. Tang, C.; Bando, Y.; Liu, B.; Golberg, D. Cerium Oxide Nanotubes Prepared from Cerium Hydroxide Nanotubes. *Adv. Mater.* **2005**, *17*, 3005–3009.
14. Wu, H.; Wei, X.; Shao, M.; Gu, J. Synthesis of Zinc Oxide Nanorods Using Carbon Nanotubes as Templates. *J. Cryst. Growth* **2004**, *265*, 184–189.
15. Yu, M.; Files, B. S.; Arepalli, S.; Ruoff, R. S. Tensile Loading of Ropes of Single Wall Carbon Nanotubes and Their Mechanical Properties. *Phys. Rev. Lett.* **2000**, *84*, 5552–5555.
16. Nishioka, K.; Niidome, Y.; Yamada, S. Photochemical Reactions of Ketones To Synthesize Gold Nanorods. *Langmuir* **2007**, *23*, 10353–10356.
17. Hochbaum, A.; Gargas, D.; Hwang, Y. J.; Yang, P. Single Crystalline Mesoporous Silicon Nanowires. *Nano Lett.* **2009**, *9*, 3550–3554.
18. Davila, L. P.; Leppert, V. J.; Bringa, E. M. The Mechanical Behavior and Nanostructure of Silica Nanowires *via* Simulations. *Scripta Mater.* **2009**, *60*, 843–846.
19. Son, S. J.; Bai, X.; Lee, S. B. Inorganic Hollow Nanoparticles and Nanotubes in Nanomedicine: Part 1. Drug/Gene Delivery Applications. *Drug Discovery Today* **2007**, *12*, 650–656.
20. Harada, M.; Adachi, M. Surfactant-Mediated Fabrication of Silica Nanotubes. *Adv. Mater.* **2000**, *12*, 839–841.
21. Whitsitt, E. A.; Barron, A. R. Silica Coated Single Walled Carbon Nanotubes. *Nano Lett.* **2003**, *3*, 775–778.
22. Chen, C.; Liu, Y.; Wu, C.; Yeh, C.; Su, M.; Wu, Y. Preparation of Fluorescent Silica Nanotubes and Their Application in Gene Delivery. *Adv. Mater.* **2005**, *17*, 404–407.
23. Hu, J. Q.; Meng, X. M.; Jiang, Y.; Lee, C. S.; Lee, S. T. Fabrication of Germanium-Filled Silica Nanotubes and Aligned Silica Nanofibers. *Adv. Mater.* **2003**, *15*, 70–73.
24. Dai, L.; Chen, X. L.; Zhang, X.; Zhou, T.; Hu, B. Coaxial ZnO/SiO_2 Nanocables Fabricated by Thermal Evaporation/Oxidation. *Appl. Phys. A: Mater. Sci. Process.* **2004**, *78*, 557–559.
25. Li, Y.; Ye, C. H.; Zhang, L. D.; Fang, X. S.; Zhang, Y. G. Novel SiO_2 Nanotubes: Synthesis from ZnS Nanowires Templates and Visible Photoluminescence at 615 nm. *Chem. Lett.* **2004**, *33*, 1638–1639.
26. Li, Y. B.; Bando, Y.; Golberg, D. Indium-Assisted Growth of Aligned Ultra-Long Silica Nanotubes. *Adv. Mater.* **2004**, *16*, 37–40.
27. Obare, S. O.; Jana, N. R.; Murphy, C. J. Preparation of Polystyrene- and Silica-Coated Gold Nanorods and Their Use as Templates for the Synthesis of Hollow Nanotubes. *Nano Lett.* **2001**, *1*, 601–603.
28. Yin, Y. D.; Lu, Y.; Sun, Y. G.; Xia, Y. N. Silver Nanowires Can Be Directly Coated with Amorphous Silica To Generate Well-Controlled Coaxial Nanocables of Silver/Silica. *Nano Lett.* **2002**, *2*, 427–430.
29. Zygmunt, J.; Krumeich, F.; Nesper, R. Novel Silica Nanotubes with a High Aspect Ratio—Synthesis and Structural Characterization. *Adv. Mater.* **2003**, *15*, 1538–1541.
30. Han, W.; Zettl, A. Coating Single-Walled Carbon Nanotubes with Tin Oxide. *Nano Lett.* **2003**, *3*, 681–683.
31. Yang, Y.; Qiu, S.; Cui, W.; Zhao, Q.; Cheng, X.; Li, R. K. Y.; Xie, X.; Mai, Y. A Facile Method To Fabricate Silica-Coated Carbon Nanotubes and Silica Nanotubes from Carbon Nanotubes Templates. *J. Mater. Sci.* **2009**, *44*, 4539–4545.
32. Zhang, Y.; Shen, Y.; Han, D.; Wang, Z.; Song, Z.; Niu, L. Reinforcement of Silica with Single-Walled Carbon Nanotubes through Covalent Functionalization. *J. Mater. Chem.* **2006**, *16*, 4592–4597.
33. Yang, C.; Park, J. S.; An, K. H.; Lim, S. C.; Seo, K.; Kim, B.; Park, K. A.; Han, S.; Park, C. Y.; Lee, Y. H. Selective Removal of Metallic Single-Walled Carbon Nanotubes with Small Diameters by Using Nitric and Sulfuric Acids. *J. Phys. Chem. B* **2005**, *109*, 19242–19248.
34. Tasis, D.; Tagmatarchis, N.; Bianco, A.; Prato., M. Chemistry of Carbon Nanotubes. *Chem. Rev.* **2006**, *106*, 1105–1136.
35. Wang, J.; Dai, J.; Yarlagadda, T. Carbon Nanotube-Conducting-Polymer Composite Nanowires. *Langmuir* **2005**, *21*, 9–12.
36. Yang, S. B.; Kong, B.-S.; Kim, D.-W.; Baek, Y.-K.; Jung, H.-T. Effect of Au Doping and Defects on the Conductivity of Single-Walled Carbon Nanotube Transparent Conducting Network Films. *J. Phys. Chem. C* **2010**, *114*, 9296–9300.
37. Dollase, W. A. The Crystal Structure at 220 °C of Orthorhombic High Tridymite from the Steinbach Meteorite. *Acta Crystallogr.* **1967**, *23*, 617–623.
38. Zhu, J.; Kim, J.; Peng, H.; Margrave, J. L.; Khabashesku, V. N.; Barrera, E. V. Improving the Dispersion and Integration of Single-Walled Carbon Nanotubes in Epoxy Composites through Functionalization. *Nano Lett.* **2003**, *3*, 1107–1113.
39. Zhang, Y.; Shen, Y.; Li, J.; Niu, L.; Dong, S.; Ivaska, A. Electrochemical Functionalization of Single-Walled Carbon Nanotubes in Large Quantities at a Room Temperature Ionic Liquid Supported Three Dimensional Network Electrode. *Langmuir* **2005**, *21*, 4797–4800.
40. Zhang, J.; Zou, H.; Quing, Q.; Yang, Y.; Li, Q.; Liu, Z.; Guo, X.; Du, Z. Effect of Chemical Oxidation on the Structure of Single-Walled Carbon Nanotubes. *J. Phys. Chem. B* **2003**, *107*, 3712–3718.
41. Zhang, Y.; Li, J.; Shen, Y.; Wang, M.; Li, J. Poly-L-lysine Functionalization of Single-Walled Carbon Nanotubes. *J. Phys. Chem. B* **2004**, *108*, 15343–15346.
42. Matthewson, M. J.; Kurkjian, C. R.; Gulati, S. T. Strength Measurement of Optical Fibers by Bending. *J. Am. Ceram. Soc.* **1986**, *69*, 815–821.

43. Tong, L.; Gattass, R. R.; Ashcom, J. B.; He, S.; Lou, J.; Shen, M.; Maxwell, I.; Mazur, E. Subwavelength-Diameter Silica Wires for Low-Loss Optical Wave Guiding. *Nature* **2003**, *426*, 816–819.